LOCAL SPREADING RATE ESTIMATION IN FORCED PLUMES

BY

PILAR LÓPEZ, ANA M. TARQUIS, BENJAMIN SKADDEN, ANIA MATULKA,

AND JOSÉ M. REDONDO

INSPIRATION: ORIGIN OF THE IDEA

Many years ago, Professor J. M. Redondo suggested to us that the entrainment coefficient was not constant.

IN MEMORY AND GRATITUDE

INDEX

1. INTRODUCTION

The study we present offers insights into the complex dynamics of forced turbulent plumes which are turbulent flows driven by both momentum and buoyancy fluxes.
These flows have significant geophysical importance, influencing dispersion processes in various natural and anthropogenic scenarios: volcanic eruptions, river plumes, ventilation systems or industrial emissions.

The analysis of these flows began with Morton et al. (1956), and all the studies aimed to determine the entrainment coefficient, a key parameter characterizing the rate of ambient fluid entrainment into the plume.
Different studies reported varied values for the entrainment coefficient, indicating its sensitivity to experimental conditions and plume characteristics (like local turbulence production, source conditions, and distance from the source).

GENERAL OBJECTIVE

A deepen research of the entrainment process in plumes by using the spreading rate.

SPECIFIC OBJECTIVES

01.

To answer the question:
What can we do if we want to obtain information from a geophysical phenomenon, such as a volcanic or submarine plume?

02.

To present a new methodology for analyzing plumes using image processing.

03.

To introduce the concept of local spreading rate coefficient.

04.

To analyze the time and spatial evolution of the local spreading rate coefficient.

2. LOCAL SPREADING RATE COEFFICIENT

The entrainment coefficient hypothesis (Morton et al., 1956) globally represent turbulence in plumes by introducing a constant coefficient α_E which defines the horizontal rate of surrounding fluid (entrainment velocity, U_E,) in terms of the vertical velocity, W:

$$\alpha e = \frac{Ue}{W}$$

The entrainment coefficient is difficult to be theoretically predicted and must be deduced from laboratory or field measurements.

For this reason, other researchers study entrainment dynamics of a plume through the spreading rate, β.

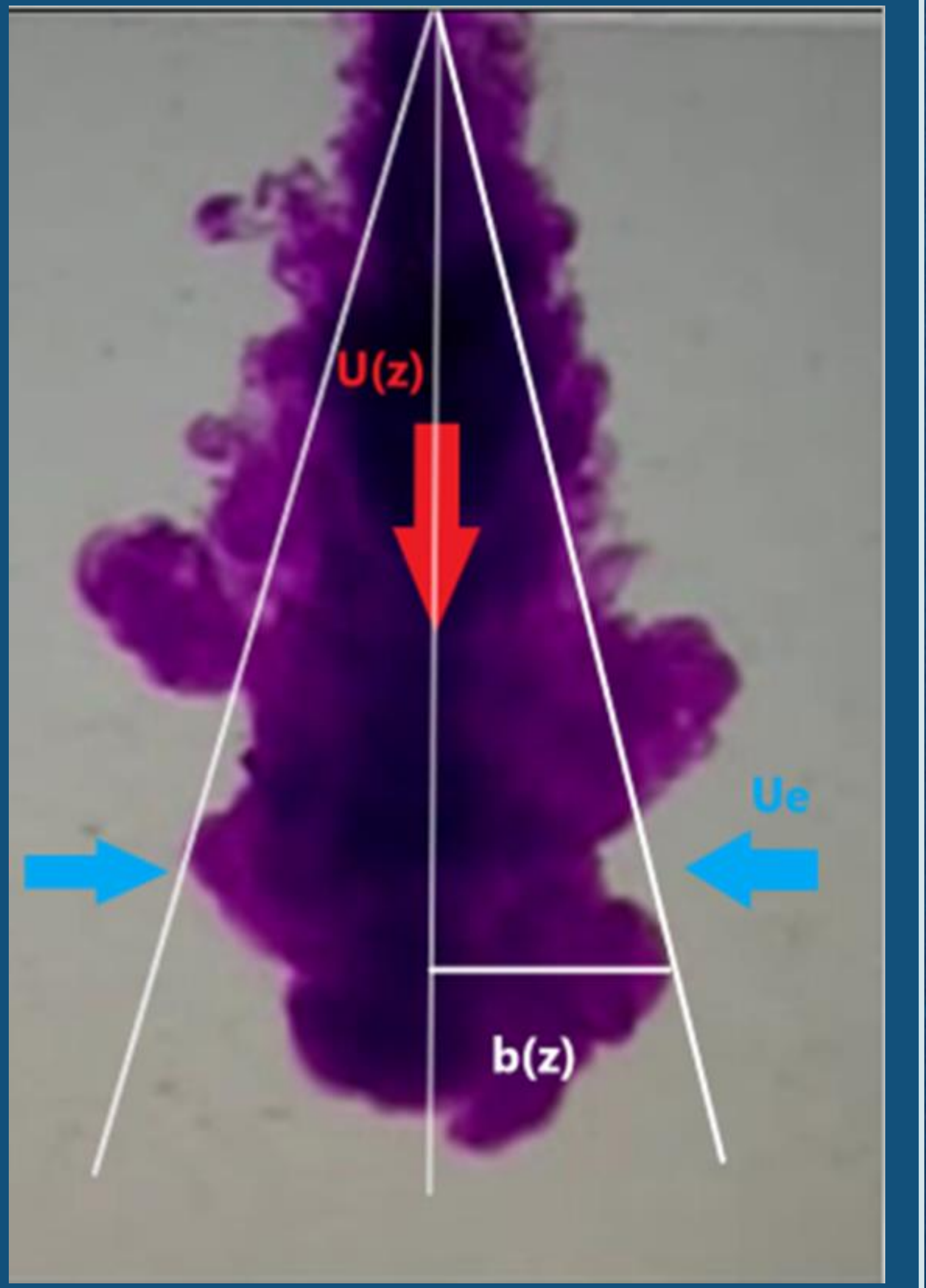

2. LOCAL SPREADING RATE COEFFICIENT

Classical and Local Spreading Rate

In a stationary ambient fluid, the Spreading Rate, β, is defined as the instantaneous rate of change of plume width, w, relative to height z, for each time or frame (the linear increase of plume width, w, relative to distance from the source, z):

$$\beta = \frac{dw}{dz}$$

Classical Spreading Rate

$$\beta_{clásico} = \frac{w_{\max}}{z_{\max}}$$

It is the quotient between the maximum width and the maximum length of the plume and it globally represents the turbulent behavior of the plume.

Local Spreading Rate

$$\beta_{local} = \frac{w_i}{z_{\max}}$$

- w_i is the width of the plume corresponding to each height z_i at a given time (as many values as heights z_i).
- Spatial and time map of the local spreading rate.
- The local spreading rate represents a percentage of the classical spreading rate at the chosen height.

3. EXPERIMENTAL SET-UP

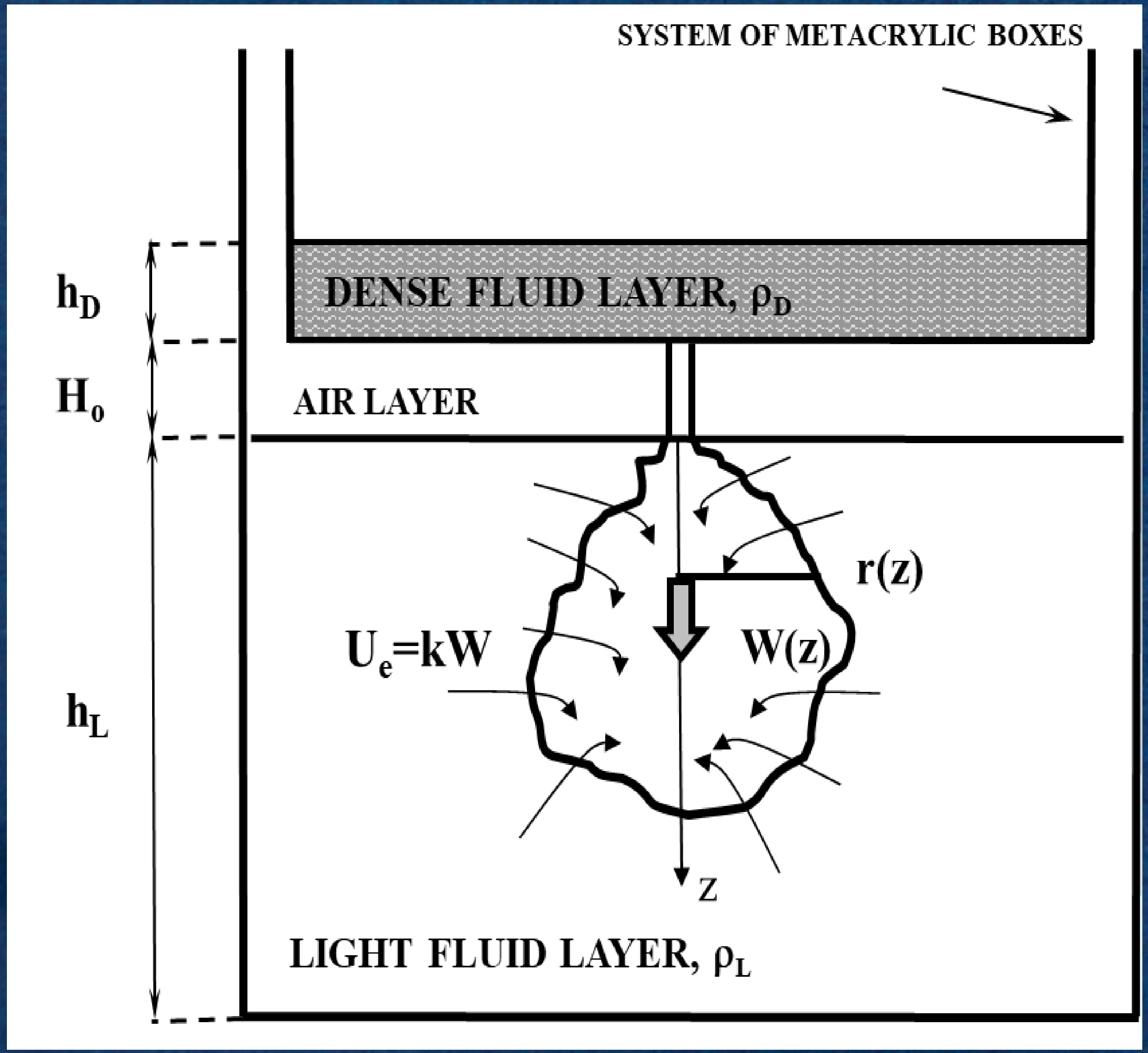

A detailed description of the experimental set-up can be found in López, Cano and Redondo (2008) and in López et al. (2017).

Outline of the experimental procedure

We outline the experimental setup for generating a turbulent forced plume in a uniform and quiet ambient fluid. The source orifice was circular with an inner diameter d = 0.6 cm and was located at a height Ho=2 cm. The turbulent plumes were produced by pumping vertically down a potassium permanganate solution of density ρD and volume 500 cm3. This denser fluid was discharged from the nozzle continuously at a flow rate of 8.40 cm3 s-1 into a glass tank containing fresh water of density ρL=1 gcm-3 at a height of 16.5 cm (height of the lighter layer, hL).
The Reynolds number at the source, based on the source diameter and the mean velocity there, is approximately 2000.

The salt solution had an intense purple colour and acted as a passive tracer. The flow was directly visualized being back illuminated by conventional fluorescents about 0.5 m from the tank.

The entering fluid is positively buoyant because the density of the plume fluid is greater than the ambient one and this unstable convective configuration enhances mixing. To characterize this density difference, we used the Atwood number, which is an indirect measure of the buoyancy. We used two different values for our experiments, A=0.001 and A=0.010.

3. EXPERIMENTAL SET-UP

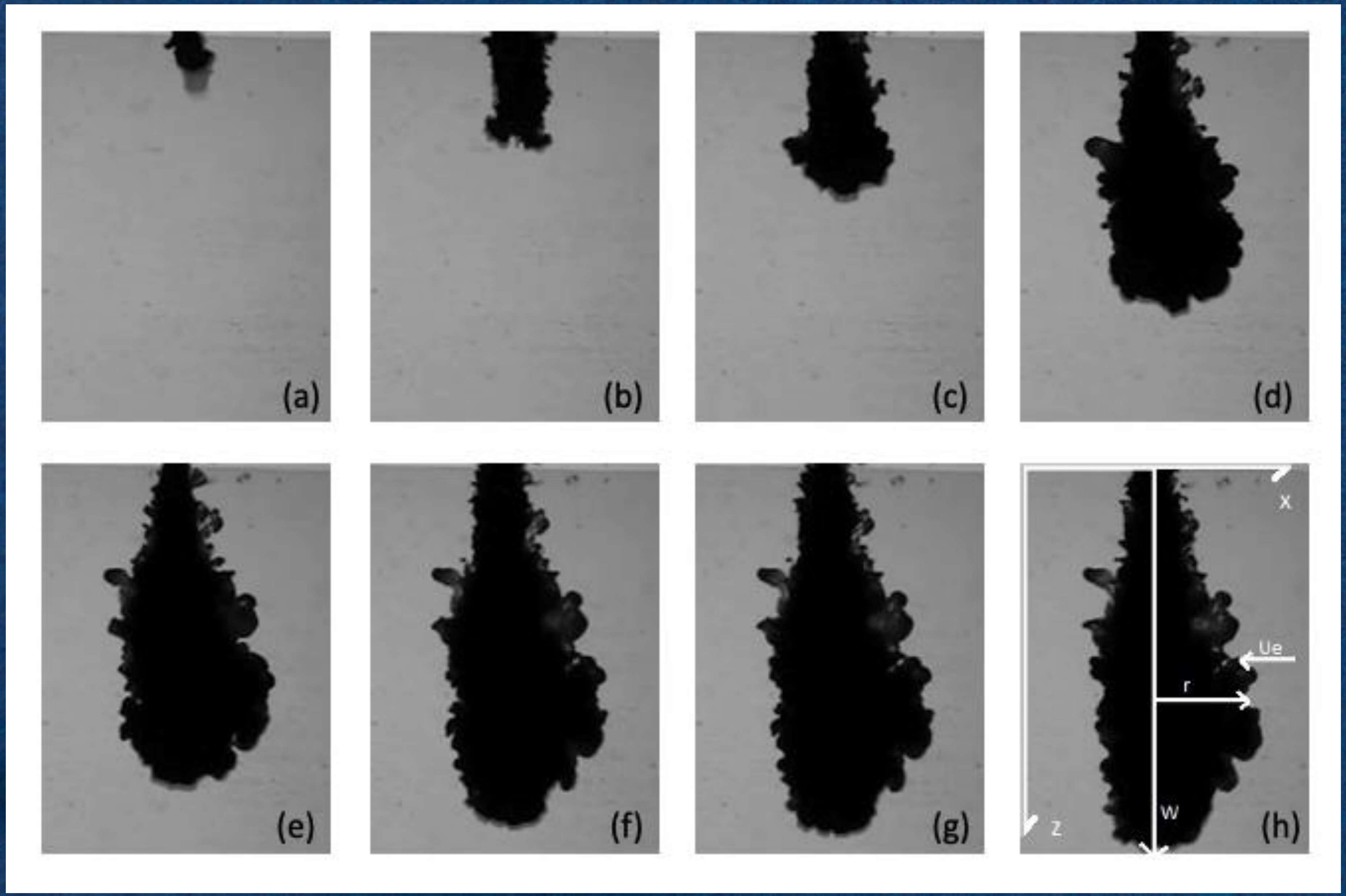

Time evolution of a plume occurring when a fluid with different density is injected into the ambient fluid for the following times: (a) 0.02 s (b) 0.07 s (c) 0.13 s (d) 0.28 s (e) 0.34 s (f) 0.38 s (g) 0.40 s (h) 0.42 s and for Atwood number $A = 0.01$ and height $H_o = 2\ cm$. The governing magnitudes in the plume where W is the axial or vertical velocity, r is the plume radius and U_e is the radial entrainment velocity at which the ambient fluid is coming into the plume.

Time evolution of a plume

The flow was captured at a rate of 100 frames per second using a high-quality digital video system. The video data was organized using frame-sequencer software (VirtualDubMod), with each frame being 640x480 pixels, covering an area of 25x18 cm^2. Intensity values for each frame ranged from 0 to 255.

4.METHODOLOGY FOR ANALYZING PLUMES USING IMAGE PROCESSING

A. MEASUREMENT PROCEDURE

01.
MatLab image conversion (color images to grayscale ones)

02.
Otsu Method (to threshold images, plume from background)

03.
MatLab programming on OTSU images (converts a frame into a matrix)

04.
Unified Matrix Type 1: the columns are the measurements of the plume length corresponding to each frame and each x-coordinate.

05.
Unified Matrix Type 2: the columns are the measurements of the plume width corresponding to each frame and each z-coordinate.

4.METHODOLOGY FOR ANALYZING PLUMES USING IMAGE PROCESSING

B. AXIAL AND RADIAL PROFILES

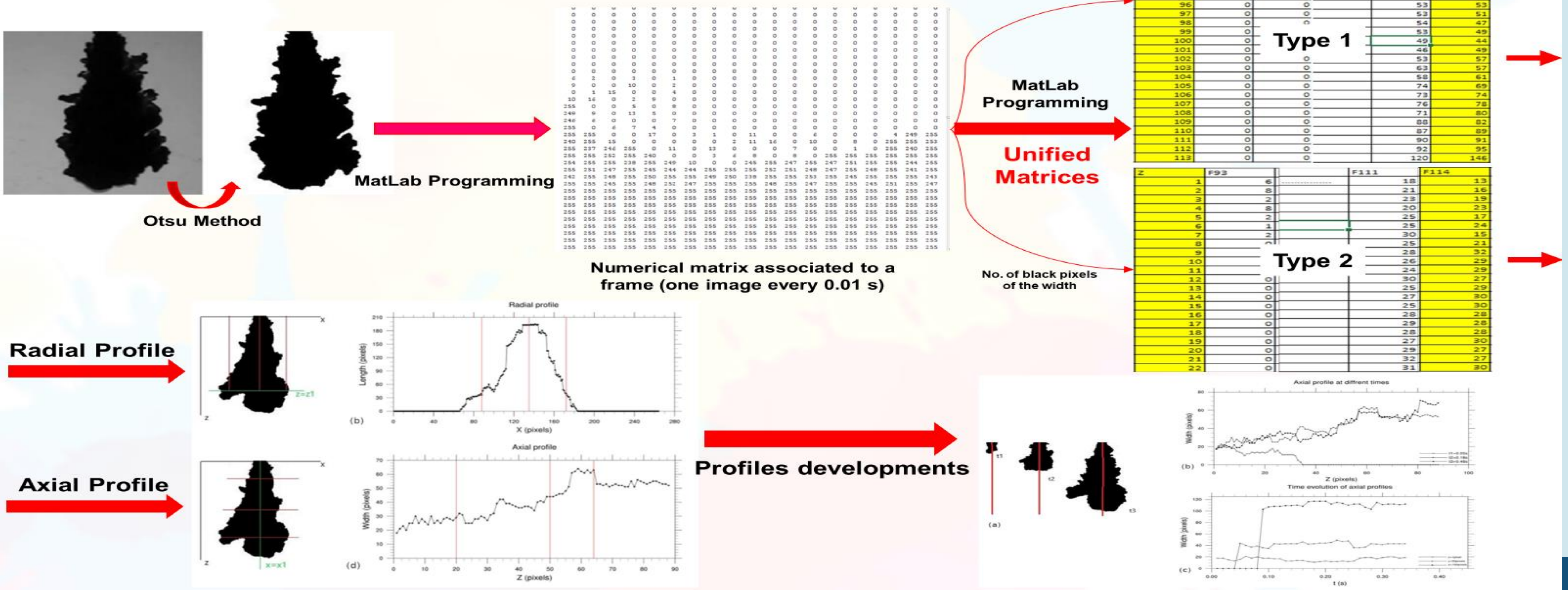

X	F93	F94	F135	F136
92	0	0	52	51
93	0	0	52	54
94	0	0	55	54
95	0	0	58	60
96	0	0	53	53
97	0	0	53	51
98	0	0	54	47
99	0		53	49
100	0		49	44
101	0		46	49
102	0	0	53	57
103	0	0	63	57
104	0	0	58	61
105	0	0	74	69
106	0	0	73	74
107	0	0	76	78
108	0	0	71	80
109	0	0	88	82
110	0	0	87	89
111	0	0	90	91
112	0	0	92	95
113	0	0	120	146

Z	F93	F111	F114
1	6	18	13
2	8	21	16
3	2	23	19
4	8	20	23
5	2	25	17
6	1	25	24
7	2	30	15
8		25	21
9		28	32
10		26	29
11		24	29
12	0	30	27
13	0	25	29
14	0	27	30
15	0	25	30
16	0	28	28
17	0	29	28
18	0	28	28
19	0	27	30
20	0	29	27
21	0	32	27
22	0	31	30

4.METHODOLOGY FOR ANALYZING PLUMES USING IMAGE PROCESSING

B. AXIAL AND RADIAL PROFILES

Unified matrix Type 1

X	F93	F94		F135	F136
92	0	0	.....	52	51
93	0	0		52	54
94	0	0		55	54
95	0	0		58	60
96	0	0		53	53
97	0	0		53	51
98	0	0		54	47
99	0	0		53	49
100	0	0		49	44
101	0	0		46	49
102	0	0		53	57
103	0	0		63	57
104	0	0		58	61
105	0	0		74	69
106	0	0		73	74
107	0	0		76	78
108	0	0		71	80
109	0	0		88	82
110	0	0		87	89
111	0	0		90	91
112	0	0		92	95
113	0	0		120	146

The radial profile illustrates how the length of a plume changes along the radial x-coordinate at a constant height (z=z1) for each time.

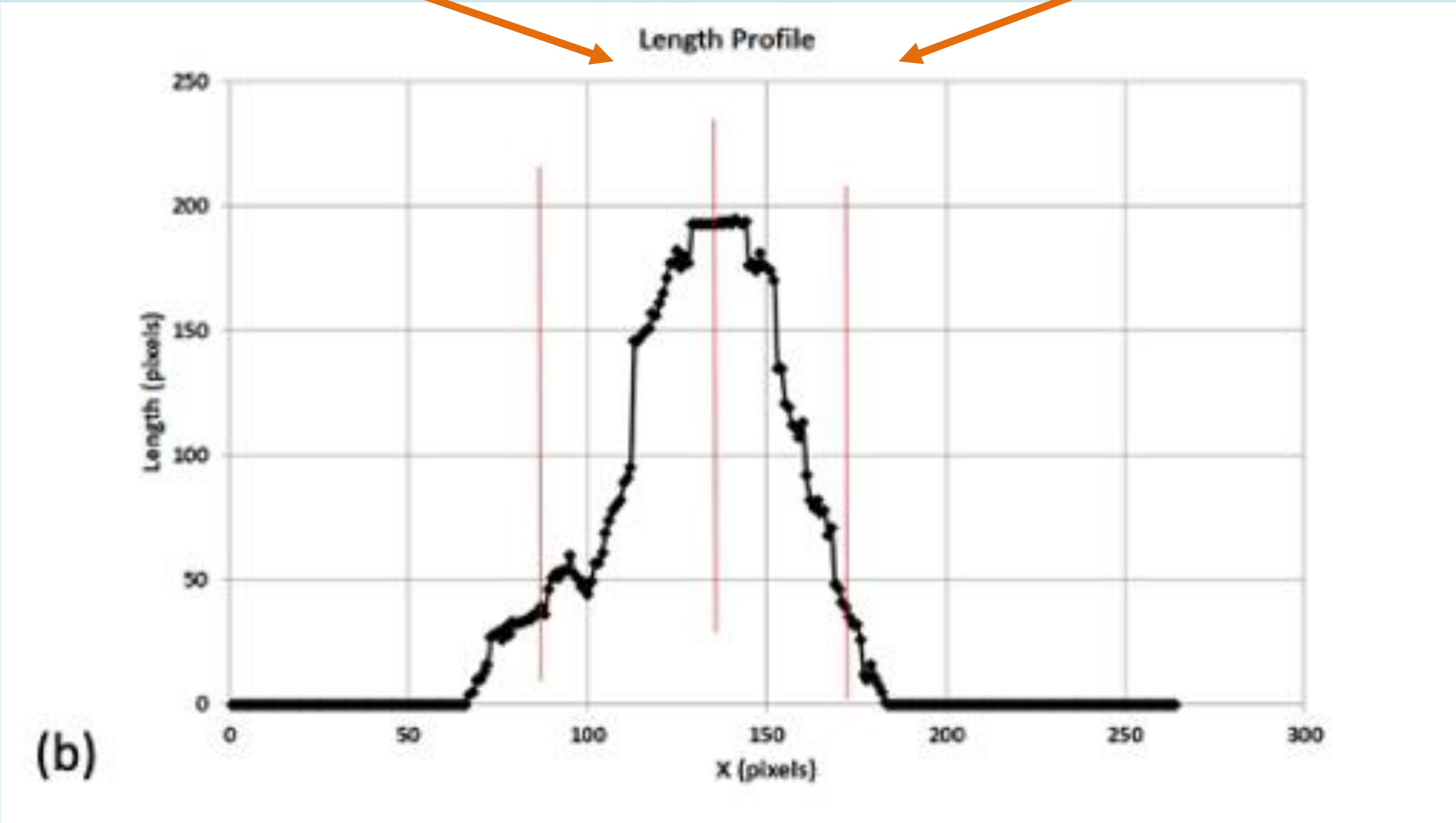

4.METHODOLOGY FOR ANALYZING PLUMES USING IMAGE PROCESSING

B. AXIAL AND RADIAL PROFILES

Unified matrix Type 2

Z	F93	F94	F95		F111	F112	F113	F114
1	6	10	18	....	18	18	15	13
2	8	11	20		21	20	17	16
3	2	11	21		23	21	18	19
4	8	7	20		20	26	20	23
5	2	10	19		25	25	22	17
6	1	7	20		25	23	22	24
7	2	5	19		30	25	21	15
8	0	5	18		25	27	22	21
9	0	5	15		28	26	26	32
10	0	6	14		26	29	29	29
11	0	5	13		24	29	25	29
12	0	5	10		30	25	24	27
13	0	4	12		25	24	23	29
14	0	3	12		27	22	26	30
15	0	5	14		25	29	24	30
16	0	5	13		28	23	24	28
17	0	4	14		29	31	29	28
18	0	6	13		28	29	30	28
19	0	4	14		27	32	33	30
20	0	8	13		29	32	32	27
21	0	6	14		32	30	31	27
22	0	6	16		31	36	29	30

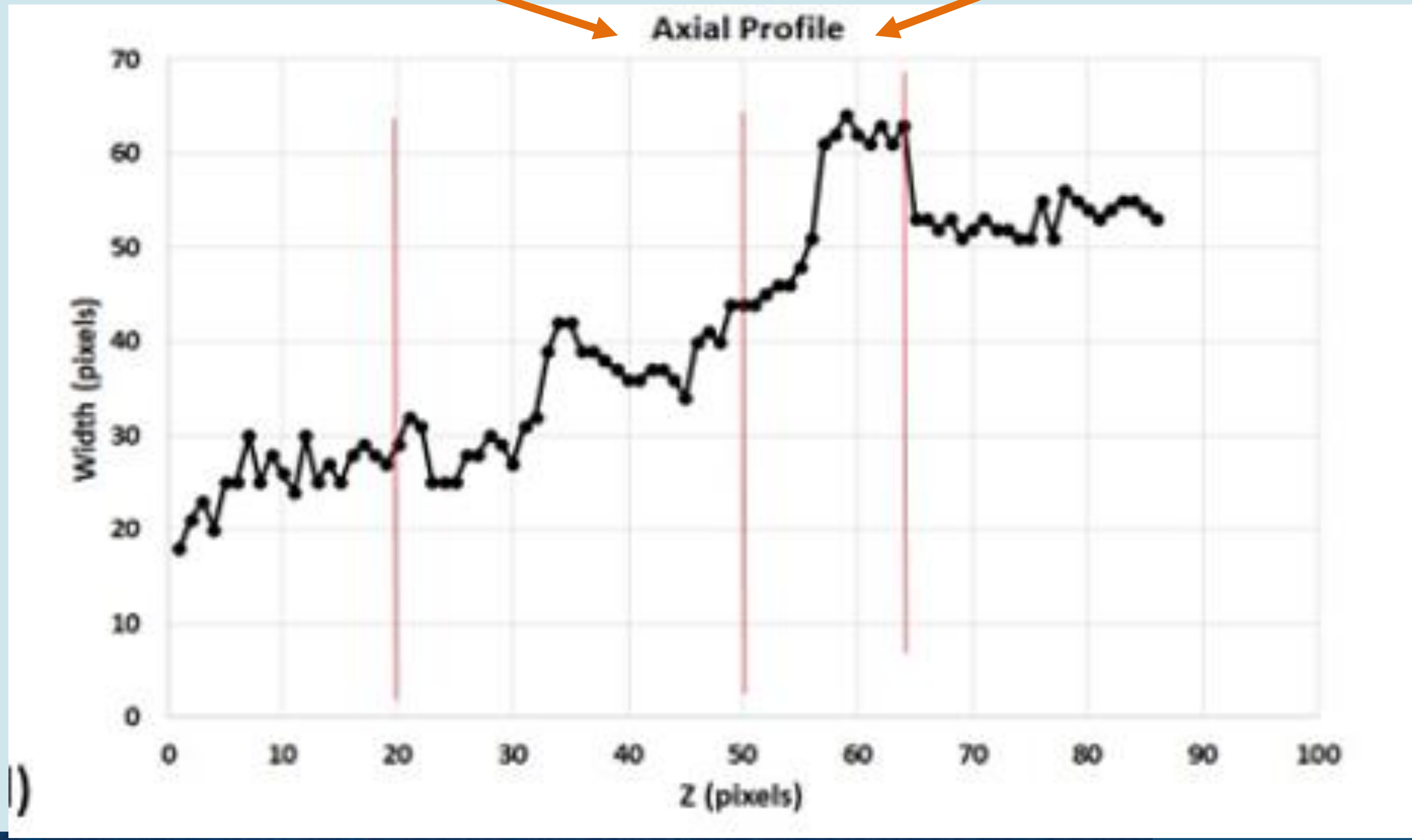

The axial profile depicts the vertical variation of the plume's width relative to the vertical z-coordinate, with x=x1 fixed, for each time.

4.METHODOLOGY FOR ANALYZING PLUMES USING IMAGE PROCESSING

C. CALCULATION OF THE LOCAL SPREADING RATE COEFFICIENT

Unified Matrix Type 2

Z	F102	F103	F104	F105	F106
1	13	13	25	28	28
2	10	10	28	26	26
3	10	10	25	25	25
4	12	12	27	28	28
5	12	12	26	28	28
6	11	11	29	29	29
7	12	12	26	28	28
8	10	10	28	32	32
9	10	10	17	32	32
10	9	9	20	29	29
11	7	7	16	27	27
12	9	9	16	26	26
13	9	9	16	26	26
14	8	8	18	26	26
15	10	10	16	26	26
16	7	7	17	27	27
17	4	4	18	29	29
18	0	0	16	26	26
19	0	0	17	27	27
20	0	0	17	27	27
21	1	1	14	29	29
22	0	0	17	27	27
23	0	0	17	28	28
24	0	0	16	27	27
25	0	0	11	24	24
26	0	0	10	24	24
27	0	0	9	21	21
28	0	0	6	22	22

Spreading rate Matrix

	t (s)	0,000	0,010	0,020	0,030	0,040	0,050	0,060
Zadim	Z	F102	F103	F104	F105	F106	F107	F108
0,00375	1	0,022	0,022	0,024	0,021	0,021	0,014	0,015
0,00749	2	0,017	0,017	0,027	0,019	0,019	0,014	0,014
0,01124	3	0,017	0,017	0,024	0,018	0,018	0,014	0,013
0,01498	4	0,021	0,021	0,026	0,021	0,021	0,014	0,014
0,01873	5	0,021	0,021	0,025	0,021	0,021	0,015	0,014
0,02247	6	0,019	0,019	0,028	0,021	0,021	0,017	0,014
0,02622	7	0,021	0,021	0,025	0,021	0,021	0,016	0,015
0,02996	8	0,017	0,017	0,027	0,024	0,024	0,017	0,015
0,03371	9	0,017	0,017	0,016	0,024	0,024	0,017	0,017
0,03745	10	0,016	0,016	0,019	0,021	0,021	0,017	0,014
0,0412	11	0,012	0,012	0,016	0,020	0,020	0,015	0,015
0,04494	12	0,016	0,016	0,016	0,019	0,019	0,016	0,015
0,04869	13	0,016	0,016	0,016	0,019	0,019	0,016	0,014
0,05243	14	0,014	0,014	0,017	0,019	0,019	0,016	0,013
0,05618	15	0,017	0,017	0,016	0,019	0,019	0,015	0,014
0,05993	16	0,012	0,012	0,016	0,020	0,020	0,014	0,013
0,06367	17	0,007	0,007	0,017	0,021	0,021	0,015	0,014
0,06742	18	0,000	0,000	0,016	0,019	0,019	0,017	0,015
0,07116	19	0,000	0,000	0,016	0,020	0,020	0,017	0,015
0,07491	20	0,000	0,000	0,016	0,020	0,020	0,016	0,015
0,07865	21	0,002	0,002	0,014	0,021	0,021	0,015	0,015

Maximum width and maximum length

	max width	13	13	29	32	32	33	39
	max z	18	18	32	42	42	56	62
	alph_Ania	0,72	0,72	0,91	0,76	0,76	0,59	0,63
	max width	0,10	0,10	0,23	0,25	0,25	0,26	0,30
	max z	0,07	0,07	0,12	0,16	0,16	0,21	0,23
t adimensional		0,00	0,02	0,03	0,05	0,06	0,08	0,10

$$\beta_{local} = \frac{w_i}{z_{\max}} \rightarrow \beta_{local} = 0.031\,\frac{n^{o}\,pixels_{black}}{z_{\max}}$$

Depth Effect Correction Coefficient

4.METHODOLOGY FOR ANALYZING PLUMES USING IMAGE PROCESSING

THIS METHOD OFFERS

1. A NON-INTRUSIVE ANALYSIS OF PLUME DYNAMICS THAT CAN BE USED IN COMPLICATED GEOPHYSICAL PHENOMENA

2. COMPREHENSIVE MEASUREMENTS ACROSS THE AXIAL AND RADIAL EXTENTS OF THE PLUME

3. A NOVEL APPROACH TO STUDYING SPATIAL EVOLUTION OF THE SPREADING RATE

5. RESULTS: APPLICATIONS

A. TIME EVOLUTION OF LOCAL SPREADING RATE COEFFICIENT

Different time behavior depending on the zone of the plume, i.e. the axial coordinate.

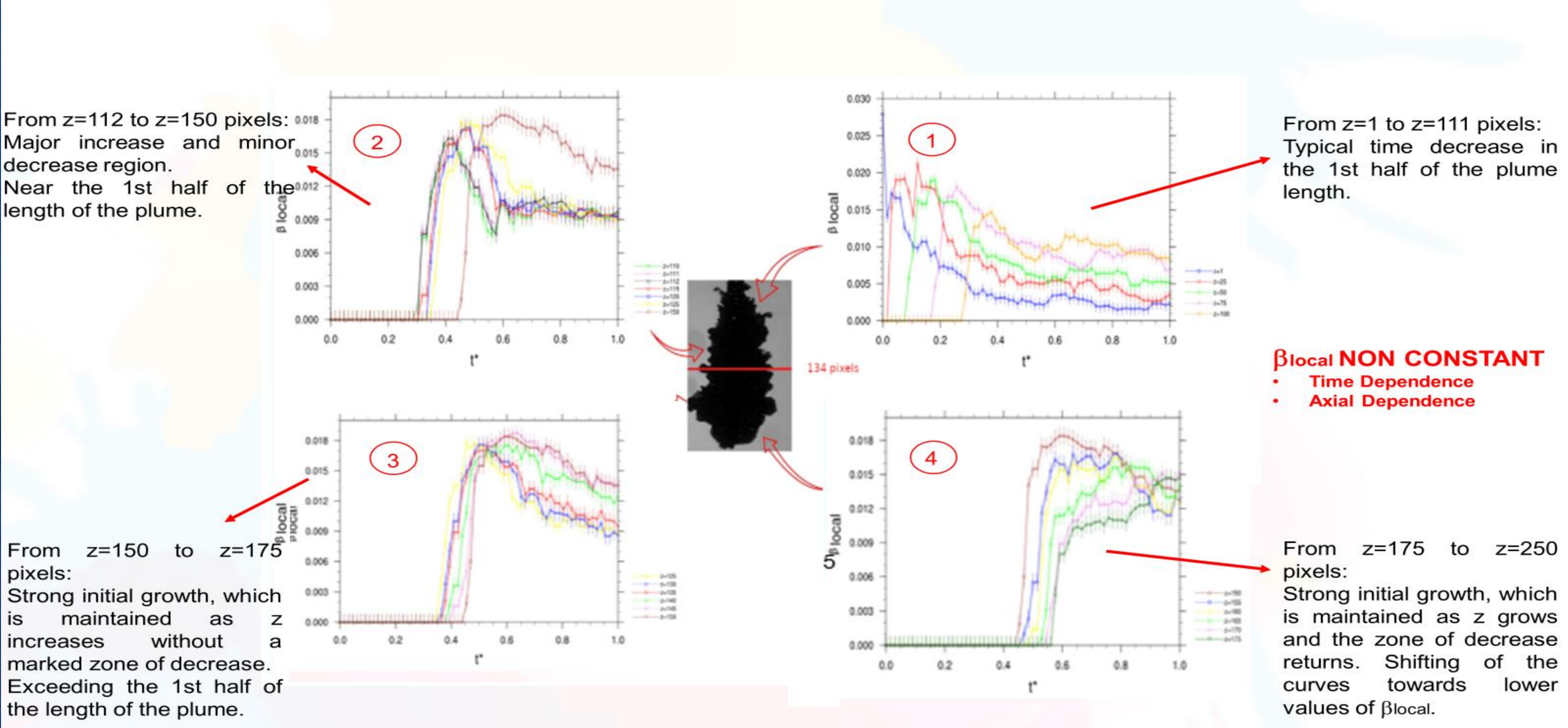

Figure clearly shows the existence of 4 areas with different behaviors when increasing depth (z):

1. Behavior Type 1: Classic
- Depths: z = 1 pixel to z = 111 pixels

2. Transition:
- At z = 112 pixels: Different behavior observed to z=150 pixels

3. Behavior Type 2:
- Depth: z = 150 pixels to z = 175 pixels

4. Final Behavior Type:
- Depths: z = 175 pixels to z = 200 pixels

5. RESULTS: APPLICATIONS

A. TIME EVOLUTION OF LOCAL SPREADING RATE COEFFICIENT

- **The initial behavior is the typical decrease over time of βlocal.**
- **This behavior occurs within the first 1/4 of the plume length.**
- **The variability in βlocal values at early times may arise from both experimental uncertainties and plume dynamics. There are greater fluctuations in the plume's concentration field near its source. With time, the concentration field becomes more uniform due to diffusion, causing βlocal to decrease and approach an asymptotic value far downstream, consistent with previous studies.**

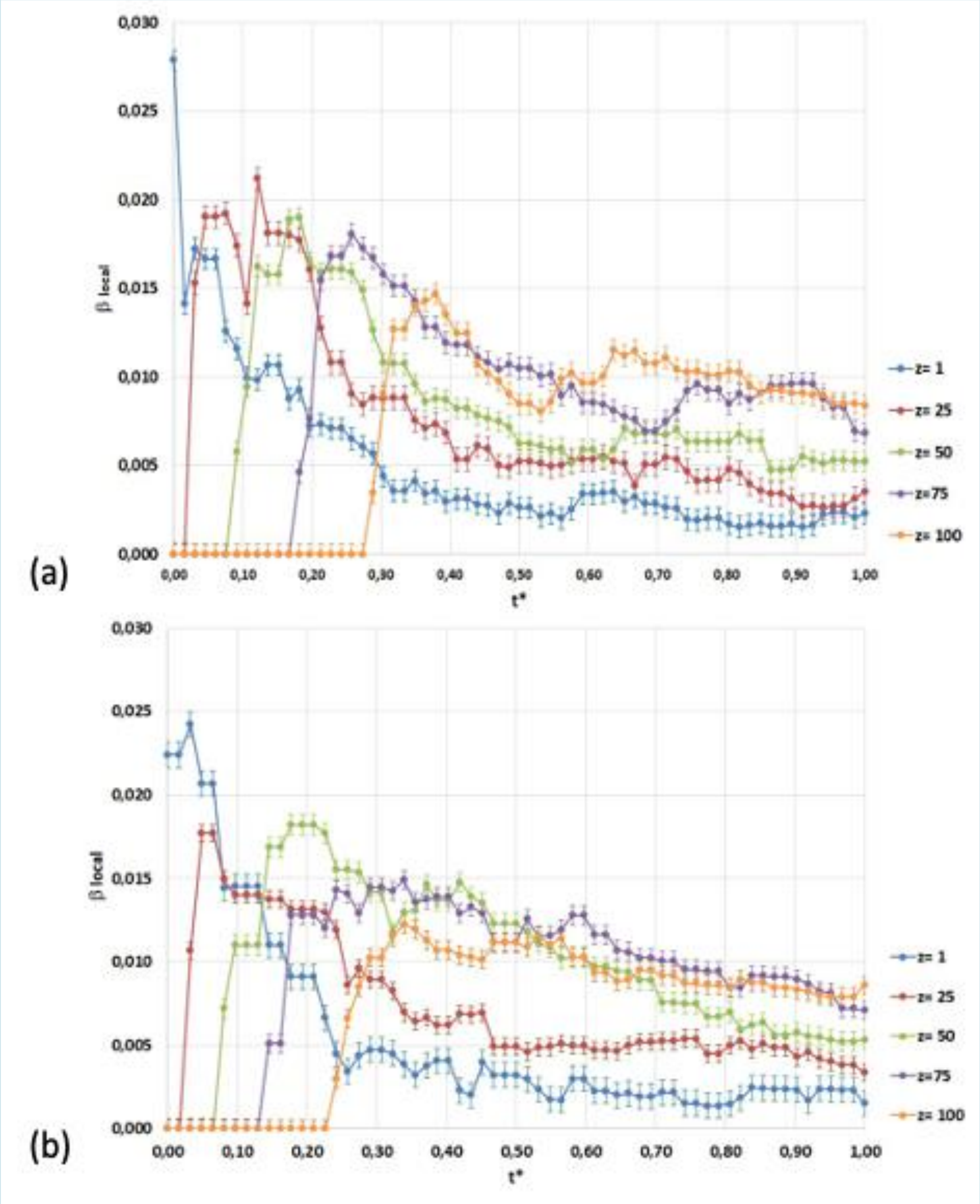

Fig. 9 Non-dimensional time evolution of the local spreading rate coefficient β_{local} at different lengt
(between *z=1 pixel* and *z=100 pixels*) for experiment with H_o= *2 cm* and (a) *A* = 0.001 (b) *A* = 0.01

- **In Figure, distinct behavior is observed compared to previous depths.**
- **For A=0.001 (Fig. 12(a)), the local spreading rate coefficient exhibits an intense growth region until reaching a peak, with subsequent smaller decrease zone, and βlocal does not decrease as significantly.**

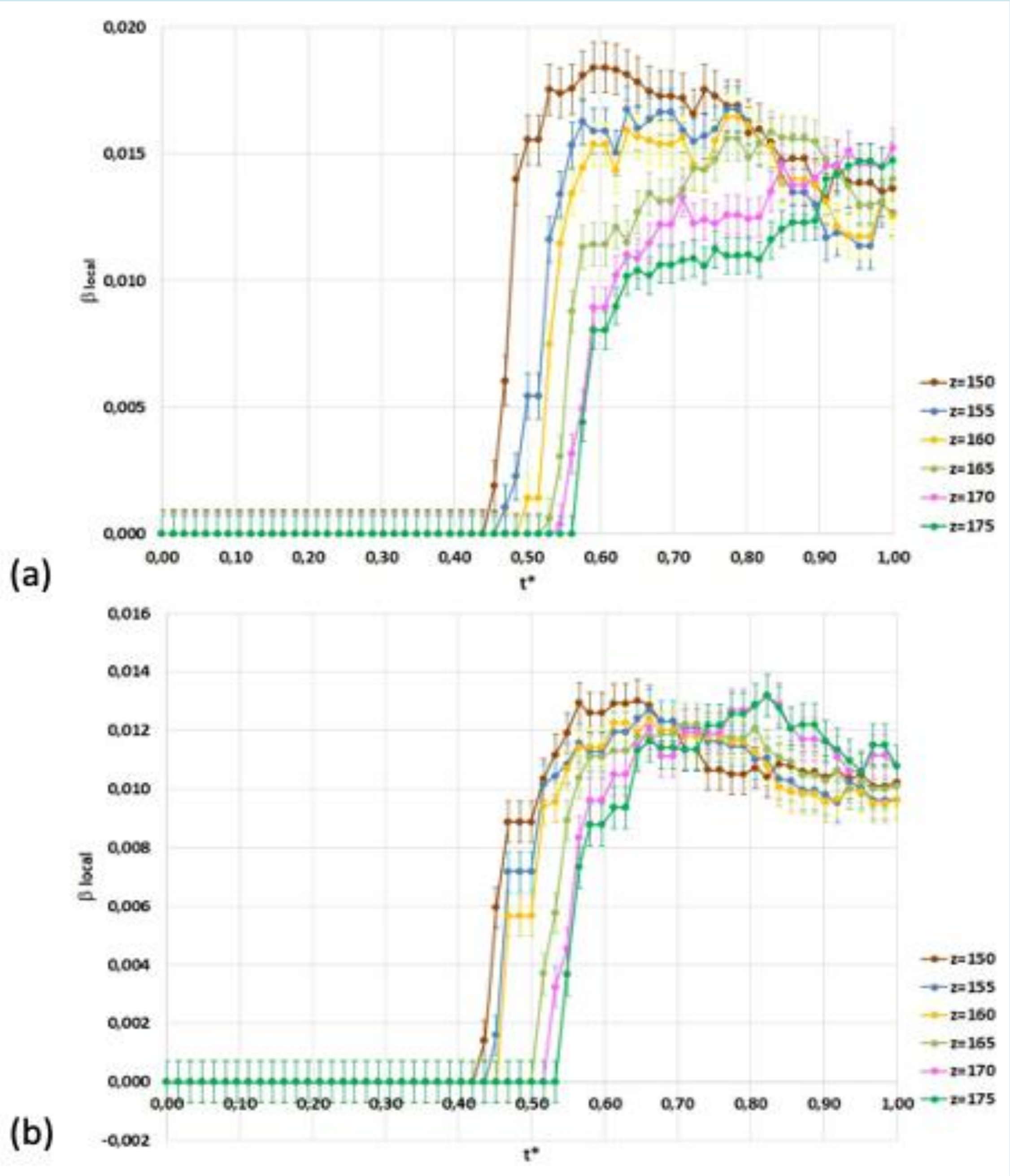

Fig. 12 Non-dimensional time evolution of the local spreading rate β_{local} between *z=150 pixels* and *z=175 pixels* for experiment with H_o= *2 cm* and (a) *A* = 0.001 (b) *A* = 0.01

5. RESULTS: APPLICATIONS

A. AXIAL EVOLUTION OF LOCAL SPREADING RATE COEFFICIENT

01.

The evolution of forced plumes is characterized by two distinct stages, as evidenced by various studies (Turner, 1973; Morton, 1959a and 1959b; Papanicolau and List, 1988; Wang and Law, 2002). Initially, forced plumes exhibit jet-like behavior, governed by momentum flux, before transitioning to plume-like behavior dominated by buoyancy.

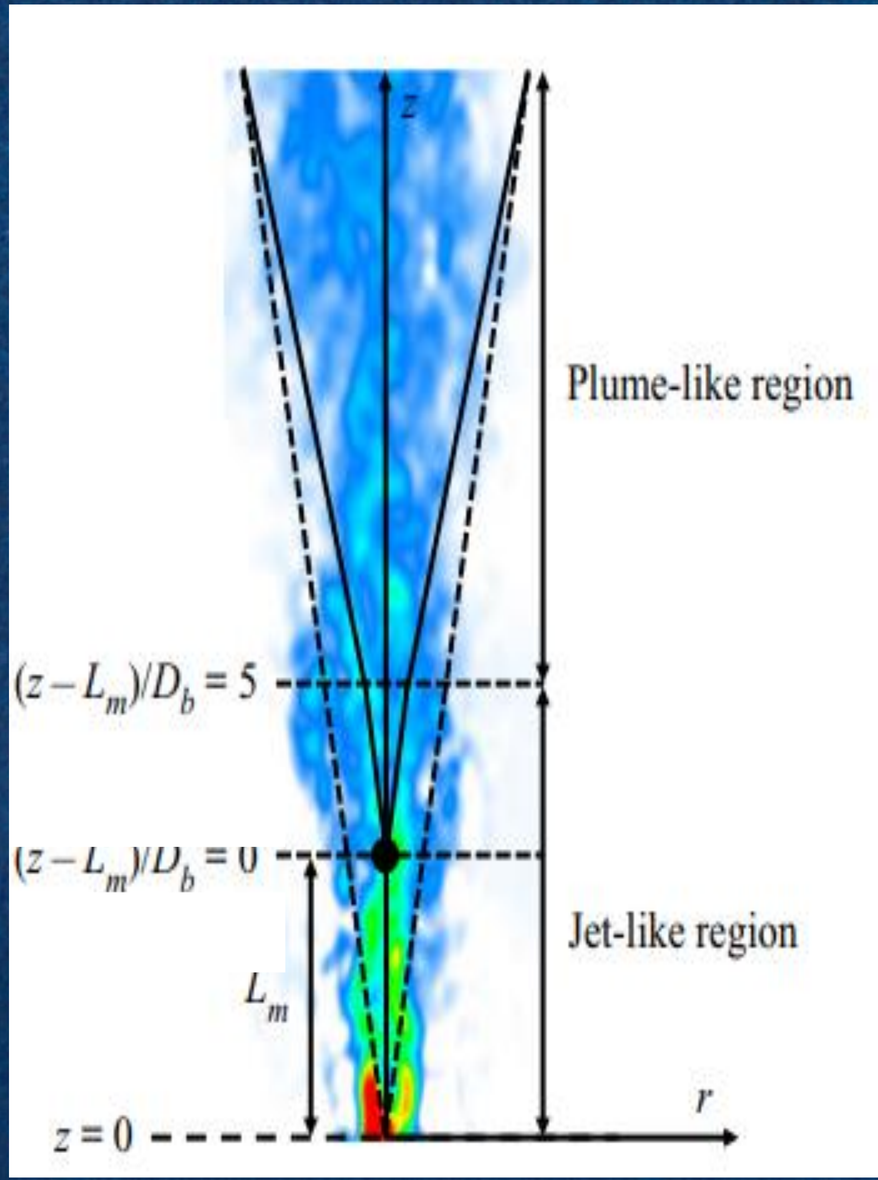

Dong Kim et al.
J. Fluid Mech. (2022), vol. 941, A42

02.

Various non-dimensional parameters, such as z/Lm, where Lm represents Fischer's characteristic length, are employed to discern whether a forced plume showcases jet-like or plume-like behavior. Typically, a forced plume is classified as a pure jet when z/Lm<0.5 and as a pure plume when z/Lm>5, with a transitional phase in between.

In the presented plume experiments, z/Lm spans from 0.165 to 1.879, indicating a transition from pure jet-like to forced plume behavior as the fluid flow's dynamical behavior is altered.

5. RESULTS: APPLICATIONS

A. AXIAL EVOLUTION OF LOCAL SPREADING RATE COEFFICIENT

This approach utilizes axial profiles where the vertical coordinate z is normalized by dividing it by the maximum depth z_{max} of the experimentally generated plume.

This transition is evident in the figure, depicting a shift from jet-like characteristics near the source to plume-like attributes further away, as indicated by the local spreading rate.

Figure shows all the axial profiles of βlocal as a function of the dimensionless depth for all times (frames) of the plume generated with A=0.001. Each curve corresponds to a time.

More specifically, there seems to be a zone of increase to the central band for both Atwood numbers and, subsequently, a decrease in the βlocal values .

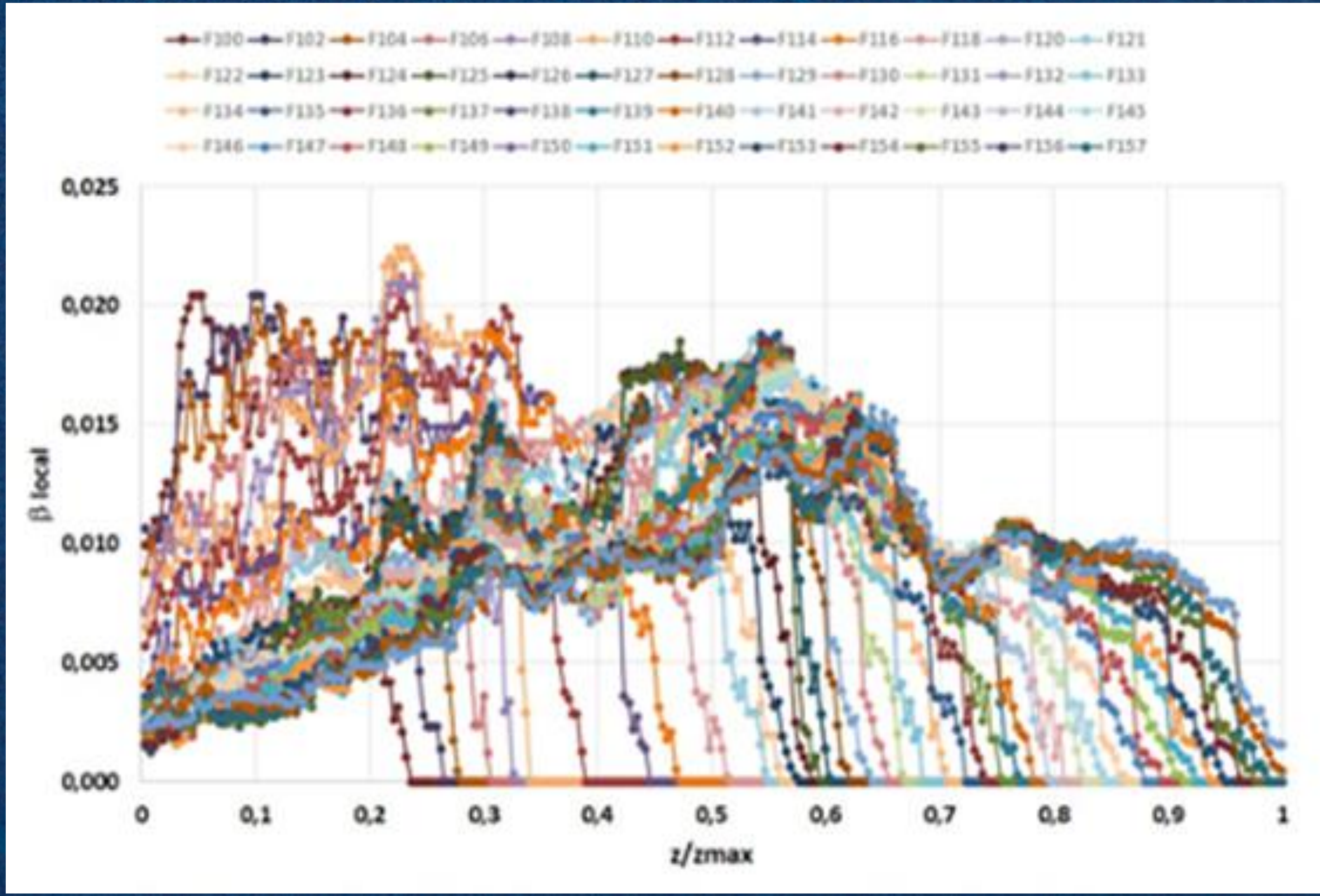

5. RESULTS: APPLICATIONS

A. AXIAL EVOLUTION OF LOCAL SPREADING RATE COEFFICIENT

To better understand where the transition from jet to plume takes place, we separate the curves corresponding to different frames in separate graphs. Figure below shows the non-dimensional vertical profiles of the local spreading rate for A=0.001 and the first half of the frames, between frames 97 and 110. :

It starts with an initial increase, the value of βlocal reaches a zone of more constant values and, later, it begins to decrease remarkably until it disappears (no existence of the plume).

This behavior implies that the local spreading rate coefficient, in addition to not being constant, presents its highest values in the central zone of the profile, with a plateau shape, which corresponds to the region of maximum width

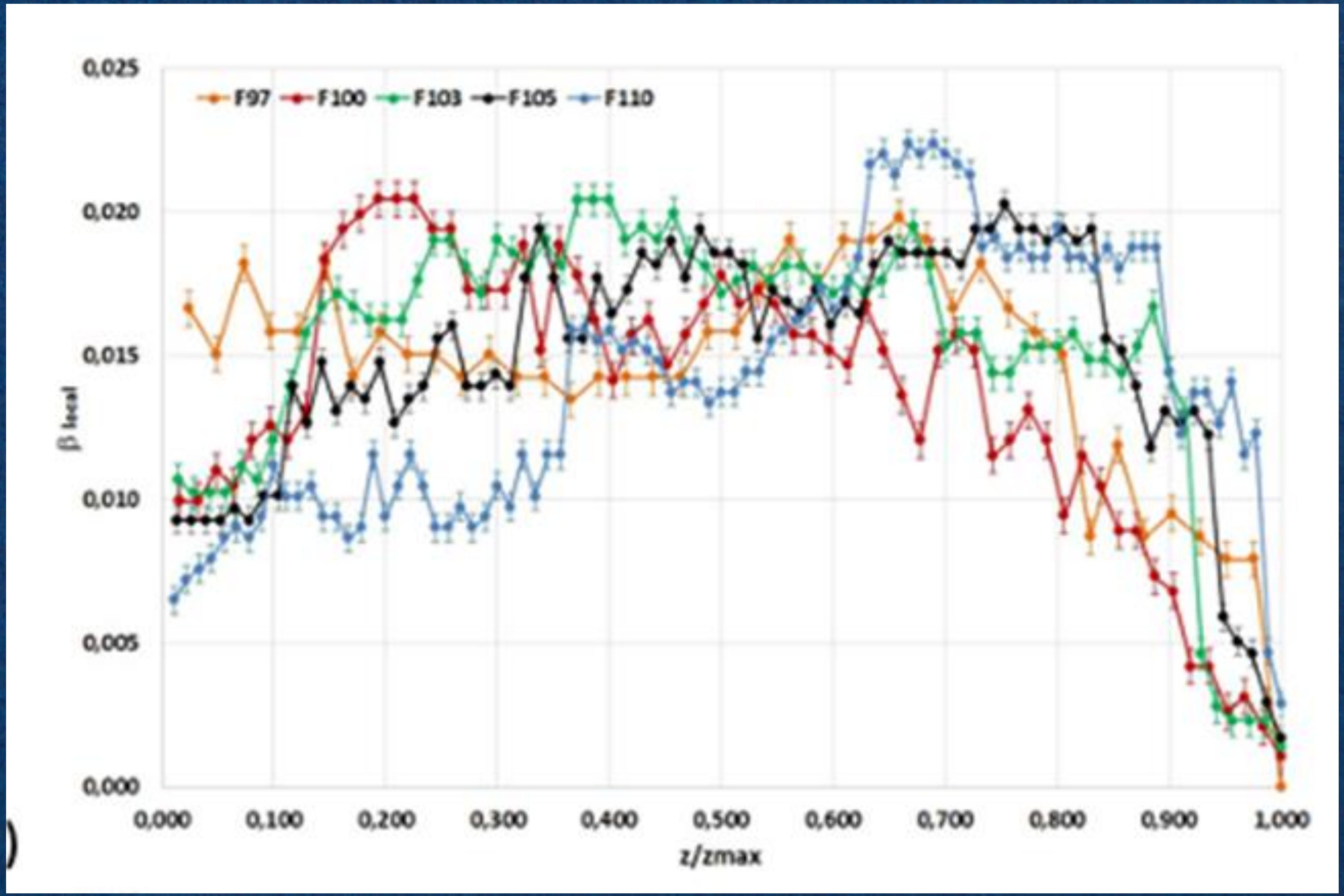

5. RESULTS: APPLICATIONS

A. AXIAL EVOLUTION OF LOCAL SPREADING RATE COEFFICIENT

To better understand where the transition from jet to plume takes place, we separate the curves corresponding to different frames in separate graphs. Figure below shows the non-dimensional vertical profiles of the local spreading rate for A=0.001 and for the second half of the frames, approximately, between frames 120 and 159:

It is observed that, again, the local coefficient βlocal varies with the dimensionless depth z/zmax, but a different behavior.

Figure shows a clear region where βlocal growths homogeneously for all times up to dimensionless depth of the order 0.4-0.5. From this depth, the growth is different for each curve or time, until the local spreading rate reaches a maximum. Following this, it begins to decrease rapidly and homogeneously for all times.

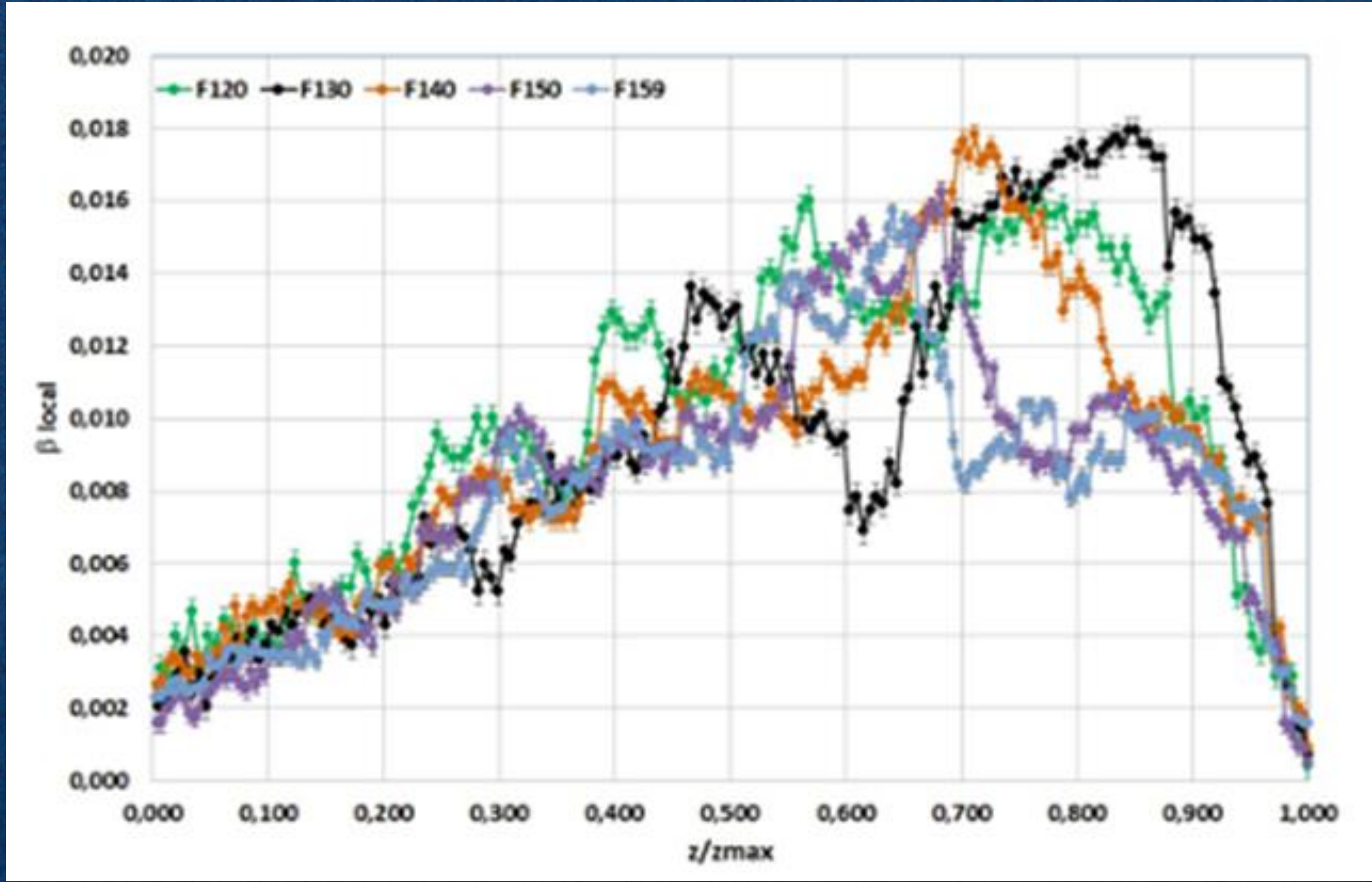

6. CONCLUSIONS

01.

Introduction of a novel methodology for analyzing the behavior of turbulent axisymmetric plumes using image data.

02.

Introduction of the local spreading rate to analyze the entrainment process, particularly its time and spatial evolutions.

03.

- The study reveals that the spreading rate coefficient is not constant, and, therefore, neither is the entrainment coefficient.
- The study confirms the variability of entrainment with distance from the source and over time.

04.

Advantages of the new methodology:

- non-invasive method
- ease of application, requiring only video recordings of fluid flows
- applicable to geophysical and anthropogenic flows (volcanic or pollution plumes)

ACKNOWLEDGMENTS

The authors express gratitude to:

- Instituto Pluridisciplinar at the University Complutense of Madrid for technical support during the experimental work.
- The support of ERCOFTAC (SIG 14).
- The study received partial funding from the European Community under project PITN-GA-2008-214919.
- It also received support from the Ministerio de Ciencia Innovación y Universidades (MCIU) under contract No. PGC2018-093854-B-I00.sos de éxito

THANK YOU FOR YOUR ATTENTION